Radiation properties of a radial line MSA array for linear polarization with stacked patch elements

Yuta Sugawara[1], Daisuke Ogawa[1], #Yuichi Kimura[1], Misao Haneishi[1], and Sakuyoshi Saito[1]
[1] Department of electrical and electronic systems, Saitama University
255 Shimo-ohkubo, Sakura-ku, Saitama-shi, Saitama 338-8570, Japan
ykimura@aplab.ees.saitama-u.ac.jp

Abstract

In this paper, a radial line microstrip antenna array (RL-MSAA) for linear polarization is designed. Stacked microstrip antennas (MSAs) with a stub element in the upper parasitic element are arrayed on a radial waveguide as a phase-controllable radiation element. A prototype array with three concentric rows of the stacked MSAs is tested in 12 GHz.

Keywords : Microstrip antenna array Stacked patch antenna Radial waveguide Stub element Phase control

1. Introduction

Microstrip antennas (MSAs) and its arrays are widely used for various applications because of small size, lightweight, low profile, and flexibility in design [1], [2]. In design of high gain MSA arrays fed by microstrip lines, gain reduction due to loss of the feeding microstrip lines should be taken into account. For this purpose, microstrip antenna arrays fed by a radial waveguide (RL-MSAA) are studied for DBS reception and other applications because transmission loss of the radial waveguide is very small [3]-[5].

Figure 1 presents a configuration of a RL-MSAA for circular polarization. MSAs are arrayed concentrically on a dielectric substrate and they are excited by a cylindrical wave in the radial waveguide via a coupling probe. Because the coupling strength to the MSA i controlled by a length of the probe, desired amplitude distribution of the MSA array is obtained. Furthermore, for circular polarization, radiation phase of the MSA is controlled by a rotation angle of the MSA orientation. However, for linear polarization, rotation of the MSA cannot be used for the phase control.

In this paper, a stacked MSA with a stub element is introduced for a linearly polarized RL-MSAA. The parasitic patch with a stub element is used for control of the radiation phase as well as wideband impedance matching. A prototype RL-MSAA with three concentric rows of the stacked MSAs are designed and tested in 12 GHz.

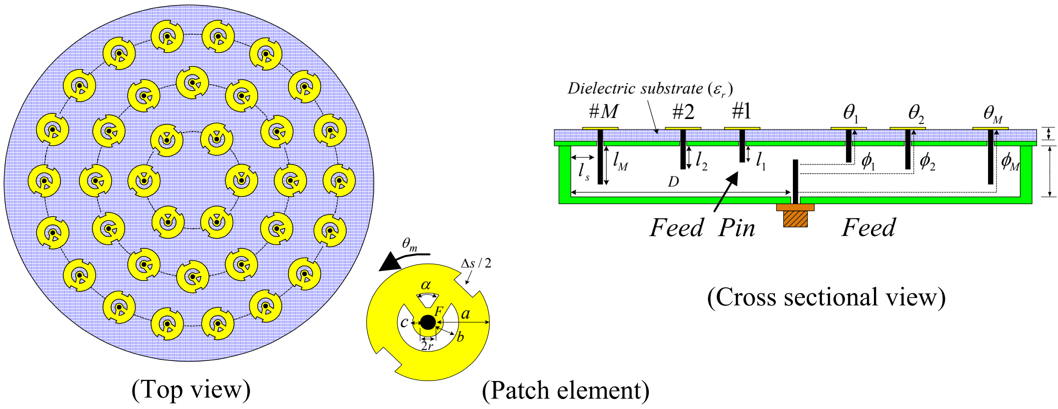

(Cross sectional view)

(Top view) (Patch element)

Figure 1: A configuration of a RL-MSAA for circular polarization.

2. A stacked MSA with a stub element

Figure 2 presents a stacked MSA with a stub element. A circular patch element is placed on the bottom dielectric substrate with a ground plane and another parasitic patch with a stub element is on the top dielectric substrate. Radiation phase of the MSA can be controlled by changing the stub length. The parasitic patch element is used in order to obtain wideband impedance performance because the resonant frequency of the MSA is varied when the stub length is changed [6]-[8].

Figure 3 presents the simulated radiation phase of the stacked MSA with the stub element when the stub length *L* is varied, where an offset of the feeding point *x* is tuned for each *L* so that good impedance matching is realized. The design frequency is 12.0 GHz and the simulation is performed by Zeland IE3D. The radiation phase can be controlled in the range of around 80 degrees. Figure 4 presents the simulated reflection of the stacked MSA. Wideband impedance characteristics are observed by the stacked configuration. The reflection is less than –10 dB when the stub length *L* is 0 to 2 mm while it is increased when *L* = 3 mm. Figure 5 presents the simulated radiation patterns of the MSA, where the stub length *L* is 2 mm. Good radiation patterns with low cross polarization are confirmed.

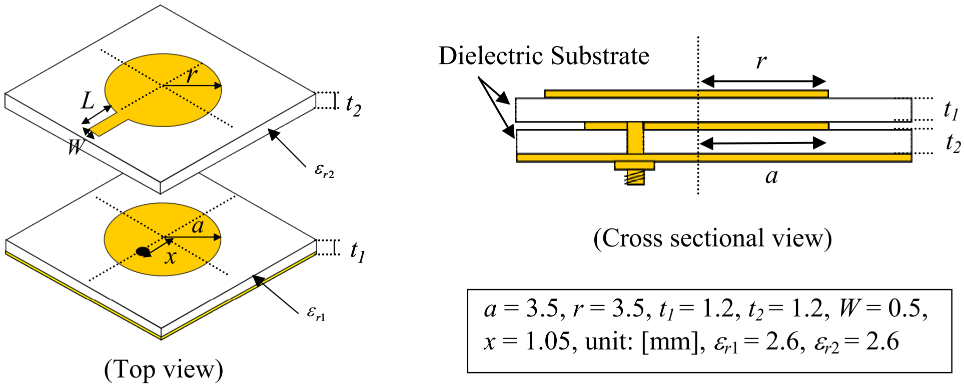

(Top view)

(Cross sectional view)

$a = 3.5$, $r = 3.5$, $t_1 = 1.2$, $t_2 = 1.2$, $W = 0.5$,
$x = 1.05$, unit: [mm], $\varepsilon_{r1} = 2.6$, $\varepsilon_{r2} = 2.6$

Figure 2: A stacked circular MSA with a stub element.

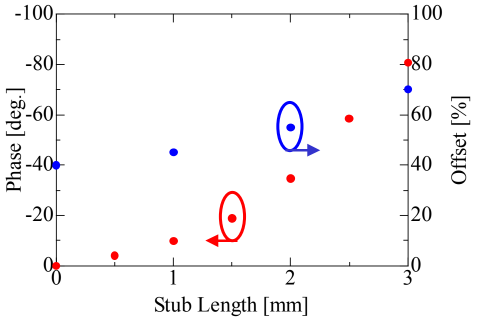

Figure 3: Simulated radiation phase of the MSA and the tuned feed point *x*.

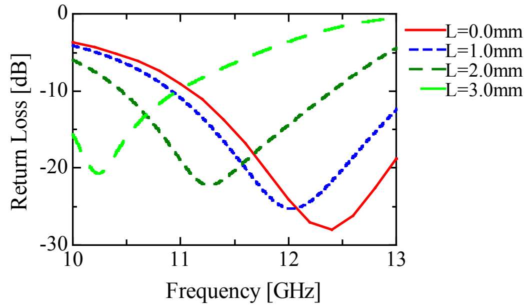

Figure 4:Simulated reflection of the MSA.

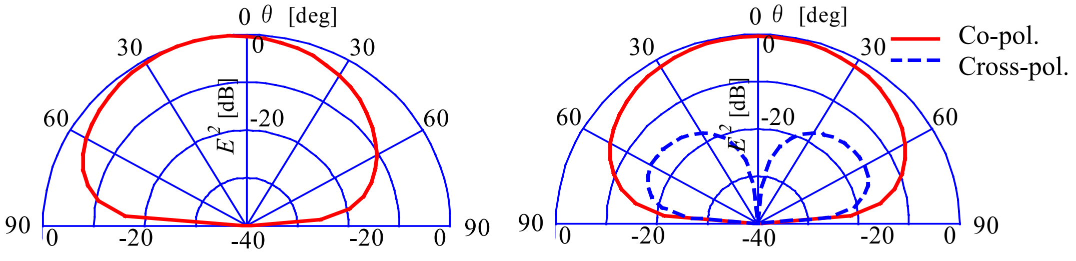

(a) E-plane.

(b) H-plane.

Figure 5: Radiation patterns of the MSA. (*L* = 2 mm)

3. Design of a RL-MSAA with the stacked MSAs

Figure 6 presents an analysis model for design of the RL-MSAA. This model is a portion of the RL-MSAA and one line of the MSAs are arranged. Port 1 is the feeding port and Port 2 to 4 are corresponding to the row 1 to 3 of the MSAs, respectively. Neighbouring MSAs are assumed on the both sides of the MSAs to simulate mutual couplings approximately in the radial waveguide. The lengths of the coupling probes l_1 to l_3 are tuned to realize uniform amplitudes by using Zealand Fidelity. Figure 7 (a) and (b) present simulated amplitudes and phases of S21 to S41, where the spacing of the MSAs are $0.65\lambda_0$. Equal amplitudes are confirmed around at 12 GHz, while different phases of S21 to S41 are observed. In order to realize uniform radiation phase of the MSAs, the stub lengths are tuned to compensate the phase differences of S21 to S41.

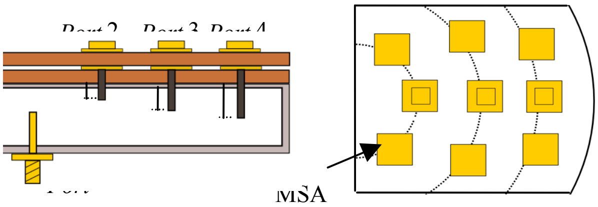

Figure 6: An analysis model of RL-MSAA for array design.

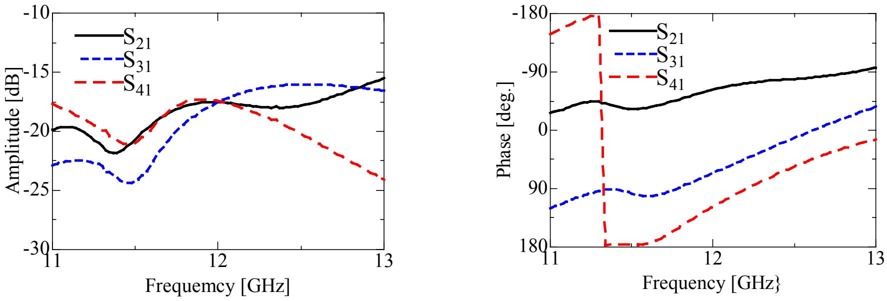

(a) Amplitude. (b) Phase.

Figure 7: Coupling distribution of the RL-MSAA with 3 rows.

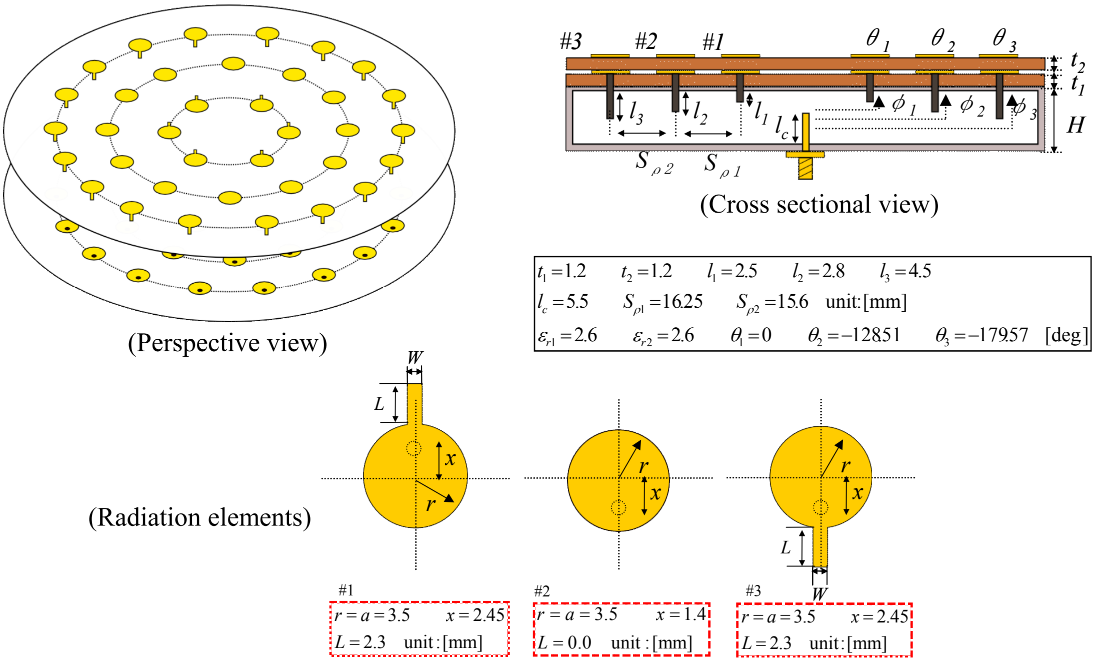

$t_1 = 1.2$ $t_2 = 1.2$ $l_1 = 2.5$ $l_2 = 2.8$ $l_3 = 4.5$
$l_c = 5.5$ $S_{\rho 1} = 16.25$ $S_{\rho 2} = 15.6$ unit:[mm]
$\varepsilon_{r1} = 2.6$ $\varepsilon_{r2} = 2.6$ $\theta_1 = 0$ $\theta_2 = -128.51$ $\theta_3 = -179.57$ [deg]

#1
$r = a = 3.5$ $x = 2.45$
$L = 2.3$ unit : [mm]

#2
$r = a = 3.5$ $x = 1.4$
$L = 0.0$ unit : [mm]

#3
$r = a = 3.5$ $x = 2.45$
$L = 2.3$ unit : [mm]

Figure 8: The testes RL-MSAA with 3 rows.

4. Experimental results of the RL-MSAA with the stacked MSAs

Figure 8 presents a prototype RL-MSAA wite 3 rows of the MSAs. The design frequency is 12.0 GHz and the spacing of the MSAs is $0.65\lambda_0$. In order to realize uniform phase distribution, the stub length and the direction of the MSAs are varied. Figure 9 presents measured reflection of the array. The reflection less than –10 dB is observed in the range of 11 to 12 GHz. Figure 10 compares the simulated and the measured radiation patterns at the design frequency. Good agreement between the simulation and the measurement is confirmed. The measured gain at 12.0 GHz is 21.6 dBi, which is corresponding to 70% efficiency.

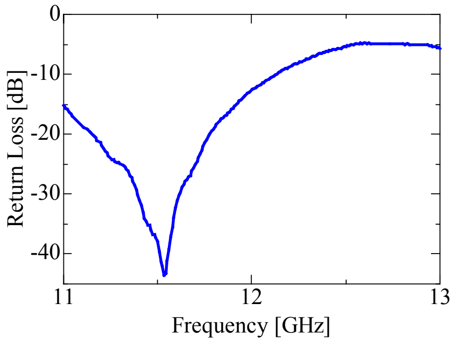

Figure 9: Reflection of the RL-MSAA.

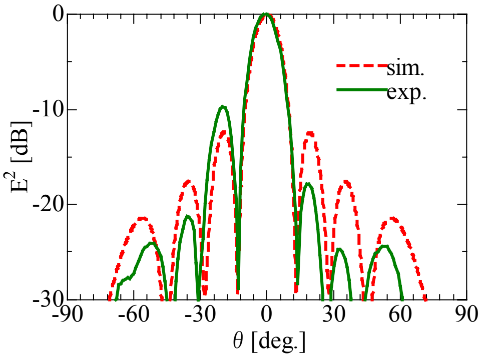

Figure 10: Radiation patterns. (f = 12.0 GHz)

5. Conclusions

This paper presents design of the RL-MSAA for linear polarization. A stacked MSA with the stub elements in the parasitic patch is introduced for the RL-MSAA. The radiation phase can be controlled by the stub length in the range of around 80 degrees. A prototype RL-MSAA with three rows of the stacked MSA is designed and tested 12 GHz. The experimental results reveal that a validity of the stacked MSA with the stub element for a linearly polarized RL-MSAA is confirmed.

References

[1] M. Haneishi, K. Hirasawa, and Y. Suzuki, *Small and planar antennas*, IEICE, 1996.

[2] M. Haneishi, “Technical features, applied technology, and perspectives of planar antenna,” IEICE Trans. (C), vol. J89-C, no. 5, pp. 198-209, May 2006.

[3] O. Shibata, S. Saito, and M. Haneishi, “Radiation properties of microstrip array antenna fed by radial line,” IEICE Trans. (B), vol. J76-B2, no. 1, pp. 20-27, Jan. 1993.

[4] K. Watanabe, M. Haneishi, Y. Kimura, and K. Nakano, “Radial-line array antenna composed of ring microstrip antennas,” IEICE Trans. (B), vol. J86-B, no. 12, pp. 2580-2584, Dec. 2003.

[5] S. Sanuki, S. Saito, Y. Kimura, and M. Haneishi, “Consideration of a radial line microstrip array antenna,” Proc. 2004 Int. Symp. Antennas Propagat., Vol. 2, pp. 1241-1244, Aug. 2004.

[6] Y. Sugawara, Y. Kimura, and M. Haneishi, “A consideration on design of a radial line microstrip array antenna,” IEICE Society Conf., B-1-96, Sep. 2008.

[7] Y. Sugawara, D. Ogawa, Y. Kimura, M. Haneishi, and S. Saito, “A consideration on design of a radial line microstrip array antenna,” IEICE Society Conf., B-1-71, Sep. 2010.

[8] Y. Sugawara, D. Ogawa, Y. Kimura, M. Haneishi, and S. Saito, “Design of a radial line MSA array for linear polarization with double-layered radiation elements,” IEICE Tech. Rep., vol. 110, no. 347, AP2010-121, pp. 19-23, Dec. 2010.